

Universal correlations of isotope effects in $Y_{1-x}Pr_xBa_2Cu_3O_{7-\delta}$

R. Khasanov,^{1,2} S. Strässle,² K. Conder,³ E. Pomjakushina,^{3,4} A. Bussmann-Holder,⁵ and H. Keller²

¹Laboratory for Muon Spin Spectroscopy, Paul Scherrer Institut, CH-5232 Villigen PSI, Switzerland

²Physik-Institut der Universität Zürich, Winterthurerstrasse 190, CH-8057 Zürich, Switzerland

³Laboratory for Developments and Methods, Paul Scherrer Institute, CH-5232 Villigen PSI, Switzerland

⁴Laboratory for Neutron Scattering, Paul Scherrer Institute and ETH Zurich, CH-5232 Villigen PSI, Switzerland

⁵Max-Planck-Institut für Festkörperforschung, Heisenbergstrasse 1, D-70569 Stuttgart, Germany

(Received 22 January 2008; published 28 March 2008)

The oxygen-isotope ($^{16}O/^{18}O$) effect on the zero-temperature superconducting energy gap Δ_0 is studied for a series of $Y_{1-x}Pr_xBa_2Cu_3O_{7-\delta}$ samples ($0.0 \leq x \leq 0.45$). In analogy to the isotope effect on the superconducting transition temperature, the isotope effect on Δ_0 increases with decreasing gap magnitude. A generic correlation between both isotope effects is established, which has been predicted from a polaronic model.

DOI: [10.1103/PhysRevB.77.104530](https://doi.org/10.1103/PhysRevB.77.104530)

PACS number(s): 74.72.Bk, 74.20.Mn, 82.20.Tr

I. INTRODUCTION

The microscopic pairing mechanism of high-temperature cuprate superconductors (HTSs) remains unknown even more than 20 years after their discovery. While for conventional superconductors the isotope effect on T_c has provided convincing evidence for a phonon-mediated pairing mechanism, the situation in HTSs is more complex, since the isotope effect is strongly doping dependent.¹⁻⁶ Especially, it is vanishingly small close to optimum doping.^{1,2} This observation has frequently been taken as evidence that the lattice is inactive in the pairing mechanism. However, with decreasing doping and decreasing T_c , the isotope effect recovers and even exceeds the BCS value of 0.5 considerably.^{1,4-6} While in conventional superconductors the isotope effect on T_c and the zero-temperature superconducting energy gap Δ_0 are intrinsically correlated, similar conclusions cannot be drawn for HTSs, especially in view of the complexity of the phase diagram and the order parameter. Thus, a systematic investigation of an isotope effect on Δ_0 can contribute to the understanding of these intricate materials.

In this paper, we report a study of the oxygen-isotope ($^{16}O/^{18}O$) effect (OIE) on Δ_0 in the cuprate superconductor $Y_{1-x}Pr_xBa_2Cu_3O_{7-\delta}$. A linear relation between Δ_0 and T_c is found as predicted theoretically. The isotope effect on Δ_0 scales linearly with the one on T_c and reverses sign around optimum doping, as anticipated from model calculations. Different doping levels of the isotope exchanged samples can be ruled out by performing careful back-exchange experiments.

II. EXPERIMENTAL DETAILS

Polycrystalline samples of $Y_{1-x}Pr_xBa_2Cu_3O_{7-\delta}$ ($x = 0.0, 0.2, 0.3, 0.45$) were prepared by standard solid state reaction.⁷ In order to obtain fine grains needed for the determination of the magnetic field penetration depth λ by low field magnetization measurements, the ceramic samples were first grounded for approximately 20 min in air and then passed through 10 μm sieves. The oxygen-isotope exchange was performed by heating the samples in $^{18}O_2$ gas. In order to ensure the same thermal history of the substituted (^{18}O)

and not substituted (^{16}O) samples, both annealings (in $^{16}O_2$ and $^{18}O_2$ gases) were always performed simultaneously. The ^{18}O content was determined from the weight change and corresponds to a 90(2)% exchange. The samples containing Pr were *c*-axis oriented in a field of 9 T, whereas samples with no Pr remained in nonoriented powder form.

ac and dc magnetization experiments were carried through in the temperature range 2–100 K by using Quantum Design magnetometers (MPMS and PPMS). The samples with no Pr were studied in dc experiments with a dc field amplitude of 0.5 mT. The oriented samples containing Pr were investigated with the ac field (field amplitude 0.3 mT and field frequency 333 Hz) applied parallel to the *c* axis. The separation of the grains and the absence of weak links were tested by confirming the linear relation between the magnetization and the field at $T = 10$ K.⁸ The dc field variation ranged from 0.5 to 1.5 mT, and the ac fields from 0.1 to 1 mT with frequencies between 49 and 599 Hz. The magnetization data were corrected by subtracting the paramagnetic background.

In Fig. 1, the magnetic susceptibility normalized to that of an ideal superconductor of spherical shape $\chi(T)/\chi_{id}$ is shown for the *c*-axis aligned ^{16}O and ^{18}O samples with $x = 0.2$. Since the ratio $\chi(T)/\chi_{id}$ is substantially smaller than 1, it is ensured that the average size of the grains is comparable to λ . This strong reduction in $\chi(T)/\chi_{id}$ is a consequence of the surface-field penetration in each individual grain. In addition, in the whole temperature range, $\chi(T)$ is systematically larger in the ^{16}O samples than in the ^{18}O samples confirming that the penetration depth is reduced in the former samples as compared to the latter ones, in agreement with previous observations.^{3-6,9,10}

In order to analyze the experimental data, we assume that the powder particles have a spherical shape and apply the Shoenberg formula¹²

$$\chi(T) = \frac{3}{2} \left[1 - \frac{3\lambda(T)}{R} \coth \frac{R}{\lambda(T)} + \frac{3\lambda^2(T)}{R^2} \right], \quad (1)$$

which relates the measured susceptibility χ to the magnetic penetration depth λ . Here, R is the average grain-size radius.

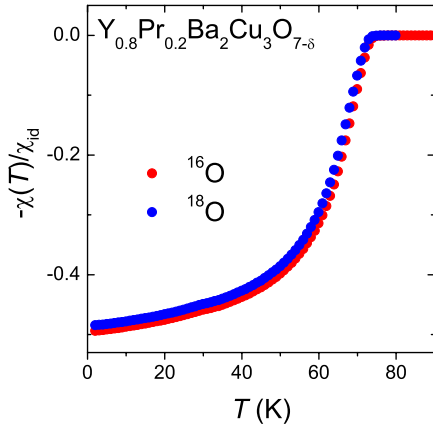


FIG. 1. (Color online) The temperature dependences of the magnetic susceptibility normalized to that for an ideal superconductor of spherical shape $\chi(T)/\chi_{id}$ for $^{16}\text{O}/^{18}\text{O}$ substituted $\text{Y}_{0.8}\text{Pr}_{0.2}\text{Ba}_2\text{Cu}_3\text{O}_{7-\delta}$.

The following issues are important for the interpretation of the experimental data: (i) When a small magnetic field is applied along the c axis, the screening currents flow in the ab plane, decaying on the distance λ_{ab} from the grain surface. Thus experiments on c -axis oriented samples provide direct information on λ_{ab} . (ii) From experiments on nonoriented powders, an effective averaged penetration depth λ_{eff} can be extracted. However, in highly anisotropic extreme type-II superconductors (as HTSs), this can—in turn—be related to the in-plane penetration depth through the relation $\lambda_{eff} \approx 1.3\lambda_{ab}$.¹³ (iii) The absolute value of λ_{ab} depends on the value of the susceptibility χ and the average grain-size radius R [see Eq. (1)], whereas the temperature dependence is independent of the grain size and entirely given by $\chi(T)$.⁸

III. EXPERIMENTAL RESULTS

The experimental results for the in-plane magnetic field penetration depth λ_{ab} for $^{16}\text{O}/^{18}\text{O}$ substituted $\text{Y}_{1-x}\text{Pr}_x\text{Ba}_2\text{Cu}_3\text{O}_{7-\delta}$ with $x=0.0, 0.2, 0.3, 0.45$ are shown in Fig. 2(a). In order to account for the undetermined average grain radius R , the values of $\lambda_{ab}^{-2}(2\text{ K})$ for the ^{16}O samples were normalized to those obtained from muon-spin rotation (μSR) experiments.¹⁴ To ensure that for the ^{16}O and ^{18}O substituted samples the doping level remained the same, back-exchange experiments were performed for two representative compositions [see Fig. 2(b)]. It is important to note here that these back-exchange experiments are absolutely essential since they guarantee that any compositional deviations or preparation errors are excluded. Only in this way can *real* isotope effects be observed in contrast to *marginal* ones caused by different doping levels.¹⁵

In the local (London) approximation ($\lambda \gg \xi$, ξ is the coherence length), the magnetic penetration depth in an anisotropic superconductor can be calculated via¹⁶

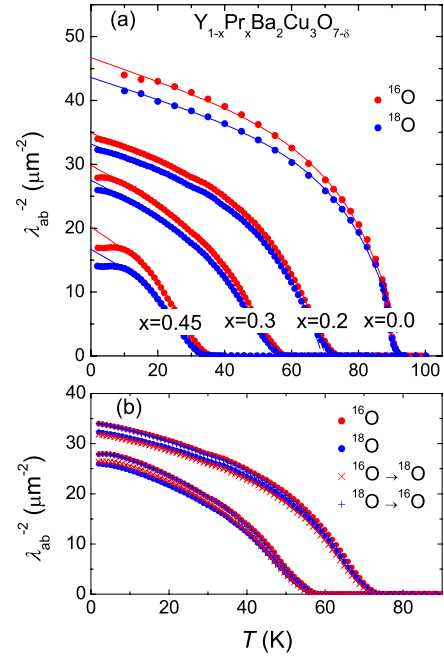


FIG. 2. (Color online) (a) Temperature dependences of the inverse-squared in-plane magnetic field penetration depth λ_{ab}^{-2} for $^{16}\text{O}/^{18}\text{O}$ substituted $\text{Y}_{1-x}\text{Pr}_x\text{Ba}_2\text{Cu}_3\text{O}_{7-\delta}$ ($x=0.0, 0.2, 0.3, 0.45$) samples. The solid lines are results from a numerical analysis as described in the text. (b) $\lambda_{ab}^{-2}(T)$ for back-exchanged ($^{16}\text{O} \rightarrow ^{18}\text{O}$, $^{18}\text{O} \rightarrow ^{16}\text{O}$) $\text{Y}_{1-x}\text{Pr}_x\text{Ba}_2\text{Cu}_3\text{O}_{7-\delta}$ ($x=0.2, 0.3$), showing that the doping level for the $^{16}\text{O}/^{18}\text{O}$ samples is unchanged.

$$\lambda_i^{-2}(T) = \frac{\mu_0 e^2}{4\pi^3 \hbar} \oint dS_F \frac{\vec{v}_i \cdot \vec{v}_i}{v_i} \left[1 + 2 \int_{\Delta_k}^{\infty} \left(\frac{\partial f}{\partial E} \right) \frac{E dE}{\sqrt{E^2 - \Delta_k^2}} \right]. \quad (2)$$

The index i refers to the principal crystallographic axes a , b , and c , v_i is the corresponding i th component of the Fermi velocity, $f = [1 + \exp(E/k_B T)]^{-1}$ is the Fermi function, Δ_k is the value of the superconducting energy gap along k , and dS_F is the Fermi surface element. The second term in Eq. (2), which is negative, describes the decrease of $\lambda_i^{-2}(T)$ caused by the thermal population of Bogoliubov quasiparticle levels with energy E . It is this quantity where the anisotropy and the magnitude of the energy gap enter. By assuming that the Fermi velocity is constant, Eq. (2) can be reduced to¹⁷

$$\frac{\lambda_i^{-2}(T)}{\lambda_i^{-2}(0)} = 1 + \frac{1}{\pi} \int_0^{2\pi} \int_{\Delta(T, \varphi)}^{\infty} \left(\frac{\partial f}{\partial E} \right) \frac{E dE d\varphi}{\sqrt{E^2 - \Delta(T, \varphi)^2}}, \quad (3)$$

where $\lambda_i^{-2}(0)$ is the zero-temperature value of the magnetic penetration depth and $\Delta(T, \varphi) = \Delta_0 s(T/T_c) g(\varphi)$. The function $g(\varphi)$ describes the angular dependence of the gap, and Δ_0 is the maximum gap value at $T=0$. The temperature dependence of the gap [$s(T/T_c)$] can either be obtained within the framework of the BCS theory extended to account for a d -wave superconductor, or by using the tabulated gap values,¹⁸ or by applying the approximate equation¹⁷

TABLE I. Values of T_c and Δ_0 for the $^{16}\text{O}/^{18}\text{O}$ substituted $\text{Y}_{1-x}\text{Pr}_x\text{Ba}_2\text{Cu}_3\text{O}_{7-\delta}$ samples investigated in this work. The relative isotope shifts of these quantities ($\delta T_c/T_c$ and $\delta\Delta_0/\Delta_0$) are given in the last two columns of the table. The values of $\delta T_c/T_c$ and $\delta\Delta_0/\Delta_0$ are corrected for the incomplete isotope exchange in the ^{18}O samples, where the ^{18}O exchange rate corresponds to 90%.

Sample	^{16}O		^{18}O		$\delta T_c/T_c$ (%)	$\delta\Delta_0/\Delta_0$ (%)
	T_c (K)	Δ_0 (meV)	T_c (K)	Δ_0 (meV)		
$\text{YBa}_2\text{Cu}_3\text{O}_{7-\delta}$	93.23(7)	29.75(22)	93.01(6)	30.06(24)	-0.26(11)	1.2(1.2)
$\text{Y}_{0.8}\text{Pr}_{0.2}\text{Ba}_2\text{Cu}_3\text{O}_{7-\delta}$	70.02(6)	19.61(14)	69.22(8)	19.33(13)	-1.27(16)	-1.6(1.1)
$\text{Y}_{0.7}\text{Pr}_{0.3}\text{Ba}_2\text{Cu}_3\text{O}_{7-\delta}$	55.50(8)	12.28(9)	54.40(8)	11.98(11)	-2.20(23)	-2.7(1.3)
$\text{Y}_{0.55}\text{Pr}_{0.45}\text{Ba}_2\text{Cu}_3\text{O}_{7-\delta}$	33.01(8)	6.87(5)	31.20(7)	6.53(5)	-6.09(37)	-5.5(1.2)
$\text{Y}_{0.8}\text{Pr}_{0.2}\text{Ba}_2\text{Cu}_3\text{O}_{7-\delta}$	69.80(6) ^a	19.54(12) ^a	69.02(7) ^b	19.19(13) ^b	-1.24(14)	-2.0(1.0)
$\text{Y}_{0.7}\text{Pr}_{0.3}\text{Ba}_2\text{Cu}_3\text{O}_{7-\delta}$	55.41(8) ^a	12.21(8) ^a	54.30(7) ^b	11.94(8) ^b	-2.23(22)	-2.5(1.0)

^aResults for back-exchanged $^{18}\text{O} \rightarrow ^{16}\text{O}$ samples.

^bResults for back-exchanged $^{16}\text{O} \rightarrow ^{18}\text{O}$ samples.

$$\Delta(T/T_c) = \Delta_0 \tanh\{1.82[1.018(T_c/T - 1)^{0.51}]\}. \quad (4)$$

We emphasize here that the temperature dependence of the gap in HTSs was found to follow the weak-coupling BCS prediction.¹⁹⁻²¹

The result of the analysis of the experimental data by means of Eq. (3), with $\Delta(T/T_c)$ described by Eq. (4) and $g(\varphi) = |\cos(2\varphi)|$ for a d -wave gap,²² are shown in Fig. 2 by solid lines. For $T > 10$ K, all experimental data are consistently described by this approach with a nearly linear temperature dependence up to $T \approx 0.5T_c$. Below 10 K, the experimental data saturate in contrast to the calculated ones which continue to increase. This deviance between experiment and theory can be a consequence of impurity scattering,²³ chemical and/or structural defects,²⁴ or may be due to the above mentioned simplifying assumption that the gap is of d -wave symmetry only. From the data, neither of these sources can be identified unambiguously. The values of T_c and Δ_0 obtained from the analysis of the $\lambda_{ab}^{-2}(T)$ data are summarized in Table I. The relative isotope shifts of T_c and Δ_0 were determined from their relative percentage change with isotope substitution. The values of $\delta T_c/T_c$ and $\delta\Delta_0/\Delta_0$ ($\delta X/X = [^{18}X - ^{16}X]/^{16}X$, $X = T_c$ or Δ_0), corrected for the incomplete isotope exchange in the ^{18}O samples, are also given in Table I. The results for the OIE on T_c are in accord with already published data.^{1,2,4-6,10,11}

In Fig. 3, the values of the zero-temperature gap Δ_0 , as determined in this study, are shown as a function of their corresponding values of T_c . In order to demonstrate their consistency with previously reported gap values, data for different HTSs, as obtained by a variety of different methods,²⁵⁻³³ are included together with theoretical results discussed below.³⁴⁻³⁶ The good agreement between the Δ_0 values of the present study with those reported in the literature implies that the above described procedure allows us to accurately determine the gap values from the measured $\lambda^{-2}(T)$. It is important to mention that even though our values of Δ_0 were derived indirectly and display some scattering (see Fig. 3), the OIE on the gap is *independent* of this methodology, since eventual errors in the absolute values of Δ_0

are systematic due to the same analysis of the data sets of ^{16}O and ^{18}O samples.

It should be outlined here that the use of Eqs. (3) and (4) in analyzing the experimental data is valid only for the case of weakly coupled BCS superconductors and does not necessarily hold for HTSs. However, the good agreement between the theoretically derived curves and the experimental ones for $T > 10$ K (see Fig. 2), as well as a good correspondence of the previously reported Δ_0 values with those observed in the present study (see Fig. 3), justifies our approach.

IV. DISCUSSION

The data presented in Fig. 3 follow a general trend, namely, Δ_0 scales almost linearly with T_c . The linear relation between Δ_0 and T_c is absolutely nontrivial, since competing and coexisting energy scales dominate the phase diagram of HTSs. Especially, the pseudogap, which is in many experiments undistinguishable from the superconducting gap, has given rise to statements controverse to our findings, i.e., that Δ_0 increases with decreasing T_c (see, e.g., Ref. 37 and references therein). The linear relation between Δ_0 and T_c was predicted by BCS theory with a value of $2\Delta_0/k_B T_c = 3.52$, smaller than observed here (see Fig. 3), which can be attributed to the d -wave gap. This linear relation obviously requires that an isotope effect on T_c results in the same isotope effect on the superconducting energy gap. However, as was outlined above, the complex symmetry of Δ_0 and the unidentified pairing mechanism do not admit any conclusions on the doping dependence of the isotope effect on the gap.

The OIE on Δ_0 is compared to the one on T_c in Fig. 4, together with theoretically derived results.³⁴ Interestingly, the same linear relation between both is observed in consistency with a model, where polaronic renormalizations of the single-particle energies were introduced.³⁴⁻³⁶ Of fundamental importance is the observation of a sign reversal of the isotope effect around optimum doping, as predicted in Refs. 34-36, which provides evidence that polaronic effects may control the physics of HTSs.

The theoretical model considers two components where the doped holes lead to the formation of metallic regions in the otherwise insulating antiferromagnetic matrix (for details, see Refs. 34–36). These holes couple strongly to the ionic displacements to form polarons with variable spatial extent. Since these metallic polaronic clusters carry huge strain fields, a self-organization into patterns (stripes) takes place which lowers the strain energy and induces interactions between the matrix and the “polaron stripes.”³⁴ The locally strong electron-lattice interaction within the metallic regions causes an *s*-wave order parameter, in contrast to the embedding matrix with a *d*-wave order parameter. Interband interactions between both subsystems guarantee a single transition temperature together with coupled gaps which were calculated self-consistently. The important effect of the polaron formation is an exponential renormalization of the bandwidth which carries an isotope effect, and an isotope independent level shift. Principally, all hopping integrals are renormalized by the polaron formation, but they contribute in a very different way to the isotope effect.³⁶ By varying the polaronic coupling, both coupled gaps, Δ_s and Δ_d , are calcu-

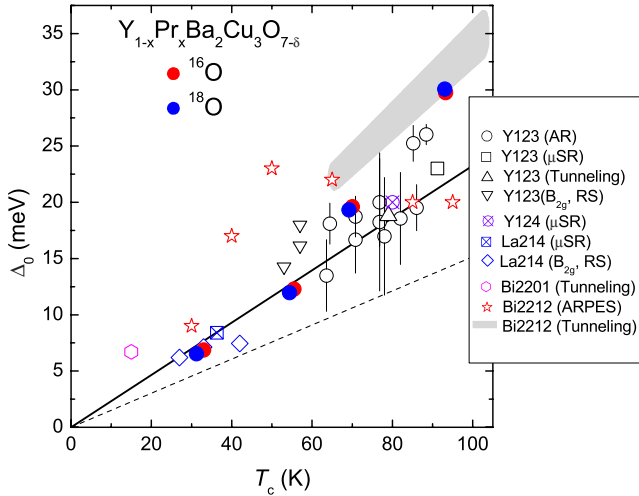


FIG. 3. (Color online) The zero-temperature superconducting gap Δ_0 vs the superconducting transition temperature T_c for $^{16}\text{O}/^{18}\text{O}$ substituted $\text{Y}_{1-x}\text{Pr}_x\text{Ba}_2\text{Cu}_3\text{O}_{7-\delta}$ samples studied in the present work and various hole-doped HTSs studied by means of Andreev reflection (AR) (Ref. 25) muon-spin rotation (μ SR) (Refs. 26–28), tunneling (Refs. 29–31), Raman scattering (RS) (Ref. 32) and angle-resolved photoemission spectroscopy (ARPES) (Ref. 33) techniques. Solid red and blue circles are the $\text{Y}_{1-x}\text{Pr}_x\text{Ba}_2\text{Cu}_3\text{O}_{7-\delta}$ data obtained in the present study (see Table I). Open circles, square, and up and down triangles are the data for $\text{YBa}_2\text{Cu}_3\text{O}_{7-\delta}$ (Refs. 25 and 28) and $\text{Y}_{1-x}\text{Ca}_x\text{Ba}_2\text{Cu}_3\text{O}_{7-\delta}$ (Ref. 29) (Y123). The crossed circle is the data point for $\text{YBa}_2\text{Cu}_4\text{O}_8$ (Y124) from Ref. 27. Open diamonds and the crossed square are the data for $\text{La}_{2-x}\text{Sr}_x\text{CuO}_4$ (La214) from Refs. 26 and 32. The open hexagon corresponds to Pb doped $\text{Bi}_2\text{Sr}_2\text{CuO}_{6+x}$ (Bi2201) (Ref. 30) and the stars represent the data for $\text{Bi}_2\text{Sr}_2\text{Ca}_{(1-x)}\text{Y}_x\text{Cu}_2\text{O}_8$ (Bi2212) (Ref. 33). The shaded gray area has been extracted from Ref. 31 where $2\Delta_0/k_B T_c = 7.9(5)$ was observed for Bi2212. The solid line corresponding to $2\Delta_0/k_B T_c = 5.34$ has been predicted theoretically by using a two-component model with polaronic coupling (Ref. 34). The dashed line corresponds to the BCS value $2\Delta_0/k_B T_c = 3.52$.

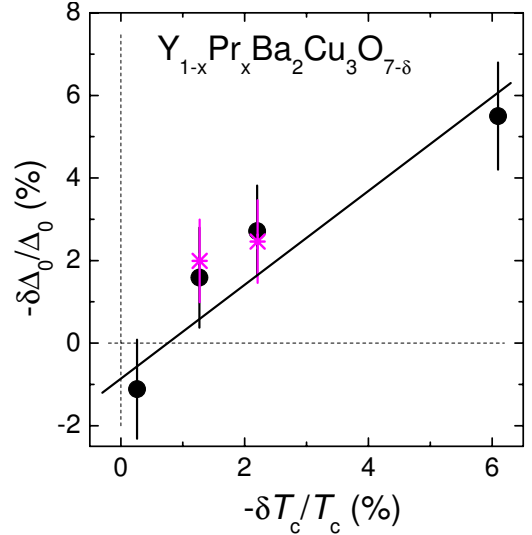


FIG. 4. (Color online) Comparison of the oxygen-isotope shift on the superconducting gap Δ_0 with the one on the transition temperature T_c for $\text{Y}_{1-x}\text{Pr}_x\text{Ba}_2\text{Cu}_3\text{O}_{7-\delta}$ ($x=0.0, 0.2, 0.3, 0.45$). The circles refer to the present experiments, and the solid line was obtained from model calculations as described in Refs. 34–36. The stars refer to the back-exchange data.

lated self-consistently for each coupling from which the average gap $\Delta_0 = \sqrt{\Delta_s^2 + \Delta_d^2}$ is obtained as a function of the corresponding T_c yielding $2\Delta_0/k_B T_c = 5.34$. These results are included in Fig. 3 as a straight line together with experimental data obtained by different techniques.^{25–33} The calculated oxygen-isotope shift of the average gap Δ_0 vs the one on T_c is compared to the present data of $\text{Y}_{1-x}\text{Pr}_x\text{Ba}_2\text{Cu}_3\text{O}_{7-\delta}$ in Fig. 4. The observed good agreement between experiment and theory is in support of polaron formation. Here, it is worth mentioning that the isotope effect on the individual gaps, i.e., Δ_s and Δ_d , is of the same order of magnitude for both gaps, but always slightly enhanced for the *d*-wave gap as compared to the *s*-wave one.³⁴ It is important to emphasize that even though our approach resembles formally the two-band BCS theory, we do not consider conventional electron-phonon coupling as the pairing interaction, but local polaron formation. This has, besides the above mentioned important band renormalizations, the additional effect of reducing the Coulomb repulsion considerably which can even become attractive. A further relevant point to mention is that the calculated isotope effect is a consequence of the renormalization of only the second and interplanar hopping integrals whereas the direct hopping integral yields the wrong tendency of the isotope effect. From these results, conclusions about the relevant displacement which causes the isotope effect can be drawn.^{34–36}

V. CONCLUSIONS

In summary, from measurements of the in-plane magnetic field penetration depth the zero-temperature superconducting energy gaps Δ_0 for $\text{Y}_{1-x}\text{Pr}_x\text{Ba}_2\text{Cu}_3\text{O}_{7-\delta}$ ($0.0 \leq x \leq 0.45$) were determined. A nontrivial linear relation between Δ_0 and T_c was found as predicted theoretically. The OIE on the super-

conducting gap Δ_0 scales linearly with the one on T_c and reverses sign around optimum doping. This sign reversal is in agreement with predictions from model calculations and unexpected from theories based on purely electronic mechanisms. Different doping levels of the isotope exchanged samples were ruled out by performing careful back-exchange experiments. The experimental results together with their theoretical analysis suggest that unconventional electron-lattice interactions play an important role in the physics of high-temperature superconductivity.

ACKNOWLEDGMENTS

The authors are grateful to K. Alex Müller for many stimulating discussions. This work was supported by the Swiss National Science Foundation, by the K. Alex Müller Foundation, and in part by the EU Project CoMePhS and the NCCR program *Materials with Novel Electronic Properties* (MaNEP) sponsored by the Swiss National Science Foundation.

- ¹J. P. Franck, J. Jung, M. A.-K. Mohamed, S. Gyax, and G. I. Sproule, Phys. Rev. B **44**, 5318 (1991); J. P. Franck, in *Physical Properties of High Temperature Superconductors IV*, edited by D. M. Ginsberg (World Scientific, Singapore, 1994), p. 189.
- ²D. Zech, H. Keller, K. Conder, E. Kaldis, E. Liarakapis, N. Poulakis, and K. A. Müller, Nature (London) **371**, 681 (1994).
- ³G.-M. Zhao, M. B. Hunt, H. Keller, and K. A. Müller, Nature (London) **385**, 236 (1997).
- ⁴G.-M. Zhao, H. Keller, and K. Conder, J. Phys.: Condens. Matter **13**, R569 (2001).
- ⁵R. Khasanov, A. Shengelaya, E. Morenzoni, K. Conder, I. M. Savić, and H. Keller, J. Phys.: Condens. Matter **16**, S4439 (2004).
- ⁶H. Keller, in *Superconductivity in Complex Systems*, edited by K. A. Müller and A. Bussmann-Holder (Springer, Berlin, 2005), p. 143.
- ⁷K. Conder, Mater. Sci. Eng., R. **32**, 41 (2001).
- ⁸C. Panagopoulos, J. R. Cooper, G. B. Peacock, I. Gameson, P. P. Edwards, W. Schmidbauer, and J. W. Hodby, Phys. Rev. B **53**, R2999 (1996).
- ⁹J. Hofer, K. Conder, T. Sasagawa, G.-M. Zhao, M. Willemin, H. Keller, and K. Kishio, Phys. Rev. Lett. **84**, 4192 (2000).
- ¹⁰R. Khasanov, A. Shengelaya, E. Morenzoni, M. Angst, K. Conder, I. M. Savić, D. Lampakis, E. Liarakapis, A. Tatsi, and H. Keller, Phys. Rev. B **68**, 220506(R) (2003).
- ¹¹R. Khasanov, D. G. Eshchenko, H. Luetkens, E. Morenzoni, T. Prokscha, A. Suter, N. Garifanov, M. Mali, J. Roos, K. Conder, and H. Keller, Phys. Rev. Lett. **92**, 057602 (2004).
- ¹²D. Shoenberg, Proc. R. Soc. London, Ser. A **175**, 49 (1940).
- ¹³V. I. Fesenko, V. N. Gorbunov, and V. P. Smilga, Physica C **176**, 551 (1991).
- ¹⁴C. L. Seaman, J. J. Neumeier, M. B. Maple, L. P. Le, G. M. Luke, B. J. Sternlieb, Y. J. Uemura, J. H. Brewer, R. Kadono, R. F. Kiefl, S. R. Krietzman, and T. M. Riseman, Phys. Rev. B **42**, 6801 (1990).
- ¹⁵A. R. Bishop, A. Bussmann-Holder, O. V. Dolgov, A. Furrer, H. Kamimura, H. Keller, R. Khasanov, R. K. Kremer, D. Manske, K. A. Müller, and A. Simon, J. Supercond. Novel Magn. **20**, 393 (2007).
- ¹⁶B. S. Chandrasekhar and D. Einzel, Ann. Phys. **505**, 535 (1993).
- ¹⁷A. Carrington and F. Manzano, Physica C **385**, 205 (2003).
- ¹⁸B. Mühlischlegel, Z. Phys. **155**, 313 (1959).
- ¹⁹K. Ichimura, K. Nomura, F. Minami, and S. Takekawa, J. Phys.: Condens. Matter **2**, 9961 (1990).
- ²⁰M. Suzuki, T. Watanabe, and A. Matsuda, Phys. Rev. Lett. **82**, 5361 (1999).
- ²¹W. S. Lee, I. M. Vishik, K. Tanaka, D. H. Lu, T. Sasagawa, N. Nagaosa, T. P. Devereaux, Z. Hussain, and Z.-X. Shen, Nature (London) **50**, 81 (2007).
- ²²G. Deutscher, Rev. Mod. Phys. **77**, 109 (2005).
- ²³P. J. Hirschfeld and N. Goldenfeld, Phys. Rev. B **48**, 4219 (1993).
- ²⁴C. Panagopoulos, W. Zhou, N. Athanassopoulou, and J. R. Cooper, Physica C **269**, 157 (1996).
- ²⁵A. Kohen, G. Leibovitch, and G. Deutscher, Phys. Rev. Lett. **90**, 207005 (2003).
- ²⁶R. Khasanov, A. Shengelaya, A. Maisuradze, F. La Mattina, A. Bussmann-Holder, H. Keller, and K. A. Müller, Phys. Rev. Lett. **98**, 057007 (2007).
- ²⁷R. Khasanov, A. Shengelaya, A. Bussmann-Holder, J. Karpinski, H. Keller, and K. A. Müller, J. Supercond. Novel Magn. **21**, 81 (2008).
- ²⁸R. Khasanov, S. Strässle, D. Di Castro, T. Masui, S. Miyasaka, S. Tajima, A. Bussmann-Holder, and H. Keller, Phys. Rev. Lett. **99**, 237601 (2007).
- ²⁹N.-C. Yeh, C.-T. Chen, G. Hammerl, J. Mannhart, A. Schmehl, C. W. Schneider, R. R. Schulz, S. Tajima, K. Yoshida, D. Garigus, and M. Strasik, Phys. Rev. Lett. **87**, 087003 (2001).
- ³⁰M. C. Boyer, W. D. Wise, K. Chatterjee, M. Yi, T. Kondo, T. Takeuchi, H. Ikuta, and E. W. Hudson, Nat. Phys. **3**, 802 (2007).
- ³¹K. K. Gomes, A. N. Pasupathy, A. Pushp, S. Ono, Y. Ando, and A. Yazdani, Nature (London) **447**, 569 (2007).
- ³²S. Sugai, H. Suzuki, Y. Takayanagi, T. Hosokawa, and N. Hayamizu, Phys. Rev. B **68**, 184504 (2003).
- ³³K. Tanaka, W. S. Lee, D. H. Lu, A. Fujimori, T. Fujii, Risdiana, I. Terasaki, D. J. Scalapino, T. P. Devereaux, Z. Hussain, and Z.-X. Shen, Science **314**, 1910 (2006).
- ³⁴A. Bussmann-Holder and H. Keller, in *Polarons in Advanced Materials*, Springer Series in Materials Science Vol. 103, edited by A. S. Alexandrov (Springer, New York, 2007), p. 599.
- ³⁵A. Bussmann-Holder, H. Keller, A. R. Bishop, A. Simon, R. Micnas, and K. A. Müller, Europhys. Lett. **72**, 423 (2005).
- ³⁶A. Bussmann-Holder and H. Keller, Eur. Phys. J. B **44**, 487 (2005).
- ³⁷Ø. Fischer, M. Kugler, I. Maggio-Aprile, C. Berthod, and C. Renner, Rev. Mod. Phys. **79**, 353 (2007).